Spectrochimica Acta Part A: Molecular and Biomolecular Spectroscopy 152 (2016) 622–628

Contents lists available at ScienceDirect

Spectrochimica Acta Part A: Molecular and Biomolecular Spectroscopy

journal homepage: www.elsevier.com/locate/saa

Analytical studies of the Alexandrovo Thracian tomb wall paintings

Z. Glavcheva [a,*], D. Yancheva [a], E. Velcheva [a], B. Stamboliyska [a], N. Petrova [b], V. Petkova [c], G. Lalev [d], V. Todorov [e]

[a] Institute of Organic Chemistry with Center of Phytochemistry, BAS, Sofia, Bulgaria
[b] Institute of Mineralogy and Crystallography, BAS, Sofia, Bulgaria
[c] New Bulgarian University, 21, Montevideo Street, Res. Quarter Ovcha Kupel, Sofia 1618, Bulgaria
[d] School of Chemistry, Cardiff University, Cardiff CF10 3AT, UK
[e] National Academy of Art, Faculty of Applied Arts, Sofia, Bulgaria

HIGHLIGHTS

- DSC, FTIR, HRTEM and EDS analysis of archaeological samples.
- Beeswax used as a binding agent in Thracian tomb wall paintings in the 4th century BC.
- Presence of Au, TiO_2 and CeO_2 nanoparticles.

GRAPHICAL ABSTRACT

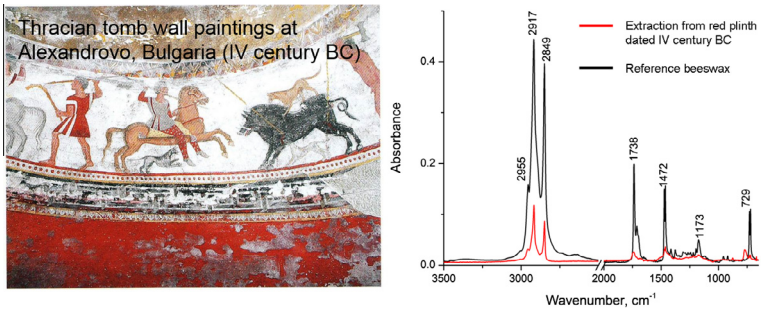

ARTICLE INFO

Article history:
Received 10 August 2014
Received in revised form 19 January 2015
Accepted 30 January 2015
Available online 8 February 2015

Keywords:
Beeswax
Archaeology
DSC
FTIR
HR-TEM
EDS

ABSTRACT

A profound study of samples obtained from Thracian tomb wall paintings at Alexandrovo, Bulgaria (dating back to the fourth century BC) were carried out by differential scanning calorimetry (DSC), Fourier transform infrared spectroscopy (FTIR) and Attenuated Total Reflectance Fourier transform infrared spectroscopy (ATR FTIR), high-resolution transmission electron microscopy (HRTEM) and energy dispersive X-ray spectroscopy (EDS). The current work provides a glimpse of the ingenious construction and painting techniques used in Thracian tomb at Alexandrovo. The results suggest that beeswax was used as a paint binder and also revealed presence of various nano-materials.

Introduction

The scientific analysis of an artwork can provide knowledge about the techniques and materials used during a specific time period and assist discovering forgeries or later repainting. The detailed knowledge of the materials composition of an artwork is an important prerequisite to carry out research in the field of art science or archaeology and to establish the proper procedures for conservation and restoration. However, a single analytical technique cannot provide complete information about the materials and techniques used in the artwork and usually complementary methods of examination and analysis have to be carried out in parallel.

* Corresponding author. Tel.: +359 2 9606 138; fax: +359 2 8700 225.
E-mail address: zornitza@orgchm.bas.bg (Z. Glavcheva).

http://dx.doi.org/10.1016/j.saa.2015.01.103
1386-1425/

The ancient Thracian tomb at Alexandrovo, Bulgaria (dated to the fourth century BC) [1] is considered as one of the most significant recent discoveries since there are very few sites with mural decoration known from this period. It holds important historical, cultural and scientific information about the religion and life of the ancient Thracians as well as about the construction and painting techniques used back then [2]. Although objects and burial remains were missing, the architecture and wall paintings are in their original state as they were made in antiquity without any conservation treatments. The interior of the tomb was originally decorated in the past. The main elements of the decoration are figurative frieze with hunting scenes which, fortunately, are completely intact (Fig. 1). At the time of discovery, part of the decoration was found fallen down and broken into pieces of different sizes. After collecting samples for analysis, only a passive conservation was carried out [3].

A life-size copy of the tomb, made in stone and having the same wall paintings, was built in a modern museum center of Thracian Art in the Eastern Rhodopes and displayed to the audience in order to ensure preservation of the original tomb.

The petrological study revealed that the tomb was made of riodacitic vitroclastic tuff stone. [3].

It is known that wax-based painting technique was used by ancient artists [4–8]. However, the composition, the way of preparation and the application of ancient wax-based paints remains subject to debate [9]. A previously reported investigation of the Thracian tomb at Alexandrovo provided preliminary information about the cross-sectional morphology of the murals [3] It was found that the paint layer was deposited on plaster made of pure slaked lime as a binder and river sand as inorganic filler. The composition of the inorganic filler is similar to the tuft – stone widespread in the Eastern Rhodopes. There are grains of quartz, sanidine, plagioclase, biotite, and amphibol [3]. The drawing was applied on the fresh wet plaster typical for the *fresco* technique which is the most frequently used technique in the Thracian wall paintings [2,4]. Due to the wetness of the plaster, an unavoidable diffusion of $Ca(HO)_2$ through the color layer took place. In the course of drying a process of carbonation occurs leading to the formation of transparent protective crust on the surface sealing the color layer [4,5].

The aim of this study is to give sufficient information about the elemental composition of the wall painting and particularly to prove the usage of beeswax in the painting techniques used by the Thracians tribes inhabited the eastern Balkan Peninsula.

Fig. 1. Fragment of the decoration in the burial chamber: hunting scene, ornamental frieze, yellow plinth (uppermost), black plinth (in the middle) and red plinth (underneath). (For interpretation of the references to color in this figure legend, the reader is referred to the web version of this article.)

Experimental

Red plinth sample from ornamental frieze (Fig. 1) was analyzed by differential scanning calorimetry (DSC), Fourier transform infrared spectroscopy (FTIR), Attenuated Total Reflectance Fourier transform infrared spectroscopy (ATR FTIR), scanning electron microscopy (SEM), high-resolution transmission electron microscopy (HRTEM) and energy dispersive X-ray spectroscopy (EDS).

The sampling method consists of two steps: firstly, the top surface protective layer of $CaCO_3$ was removed with scalpel knife in order to expose the clean surface of the paint.

The actual sample taken for analysis was prepared by scraping off the red color layer. This was carefully executed in order to avoid contamination from the plaster substrate. The obtained powder sample was divided into four parts for DSC, FTIR, HR-TEM and EDS analyses.

Differential scanning calorimetry (DSC) analysis was carried out using a SETSYS-2400 Evolution TG-DSC apparatus (SETARAM, France) under the following conditions: temperature interval: from room temperature to 200 °C, temperature heating rate of 10 °C min^{-1} and static air atmosphere. Individual samples (~8.5 mg) were placed in platinum pans. Data processing was performed by specializing CALISTO software for thermal analyses.

The FTIR and ATR-FTIR spectra were recorded on Bruker Tensor 27 FT spectrometer at a resolution of 2 cm^{-1} and 64 scans. The samples were measured in solid state (KBr pellet) and for ATR technique they were directly applied on a ZnSe crystal.

It is quite challenging task to analyze the composition of the paint binder since the quantity of the investigated samples is very small. The binder of the sample was extracted with chloroform. Commercially available spectral quality chloroform was used as solvent. After having been kept for two days at room temperature, the extracted solution was applied with micropipette on a ZnSe crystal. The chloroform was then evaporated in a draught of hot air. In this way, very thin (almost invisible) film of binder was obtained on the surface of ZnSe crystal.

To provide detailed morphological and compositional information about the studied sample at micro and nano-scale HR-TEM (LaB6) JEOL 2100 is employed. The system is equipped with high-resolution Gatan digital camera providing resolution of 0.2 Å which makes possible detailed observation of the crystal lattice, obtaining diffraction pattern and accurate measurement of the lattice d-spacing with the help of Digital Micrograph software. In scanning transmission electron microscopy (STEM) mode, dark field (HAADF/Z-contrast) detector is used to provide excellent compositional contrast. EDS system Oxford Instruments equipped with a large-area 80 mm^2 SDD (Silicon Drift Detector) X-Max^N 80 T is employed to study the elemental composition in Point&ID, LineScans, layered and elemental mapping modes. To analyze the EDS data, the latest version of AZtecTEM software is utilized.

For HR-TEM analysis, the samples were grinded and after preparing a water suspension, a drop of about 8 μL was put on the TEM grid and dried.

Results and discussion

Analysis of the paint binder by DSC and FTIR

The previous study indicated that the paint binder might contain beeswax [3]. In order to confirm this hypothesis, DSC and FTIR analyses were carried out. Both methods have been used to identify waxes and they appear to be very suitable techniques for such investigation. [7,10–16].

The beeswax is translucent solid substance that melts easily. Standard melting point analysis only partially describes the

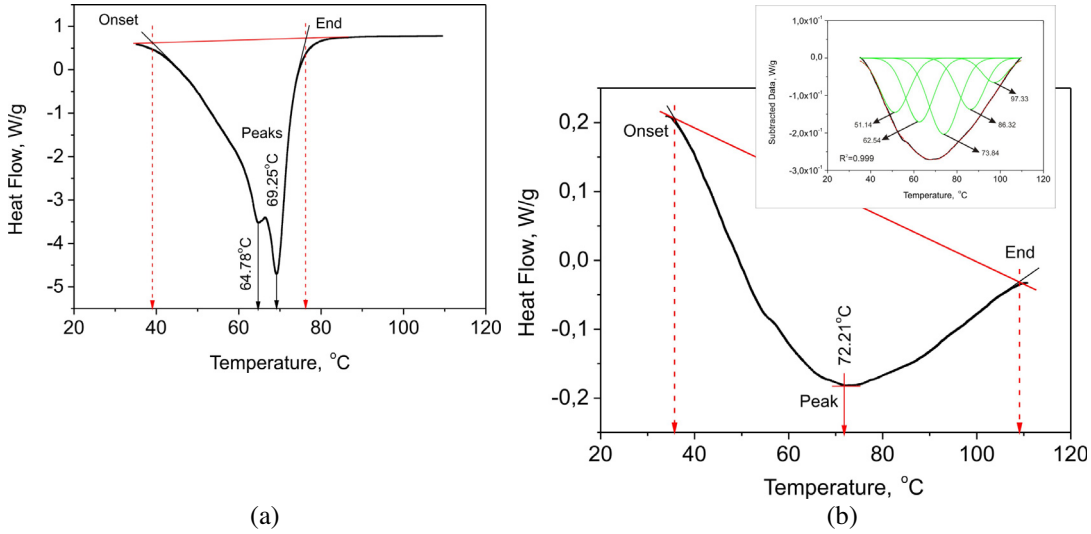

Fig. 2. DSC of reference beeswax (a) and beeswax in the red plinth (b). (For interpretation of the references to color in this figure legend, the reader is referred to the web version of this article.)

Table 1
Thermal properties of beeswaxes analyzed using differential scanning calorimetry.

No.	Species	Onset, (°C)	End, (°C)	$Peaks_{max}$, (°C)	Heat of fusion, (J/g)
1	Red plinth	35.68	109.10	72.21	59.71
2	Referent	39.04	76.28	I-64.78; II-69.25	390.77

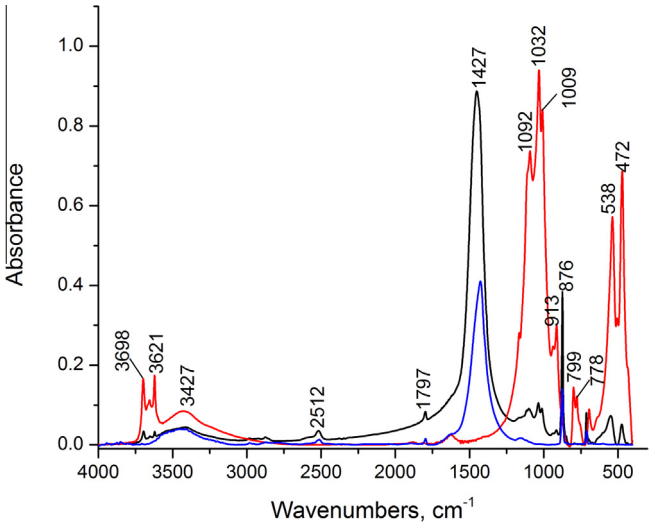

Fig. 3. FTIR spectra (KBr pellet) of red plinth sample (black line); standard $CaCO_3$ (blue line) and standard red ochre (red line). (For interpretation of the references to color in this figure legend, the reader is referred to the web version of this article.)

thermal properties of beeswaxes while DSC is a method that allows quantitative characterization of phase transitions such as melting. DSC enables determination of the temperatures over which melting occurs as well as the amount of energy associated with the melting transition, i.e., the heat of fusion [11]. Beeswaxes melt at about 64 °C and this melting point remains fairly constant with ageing. It has been shown as well that impurities and mixtures broaden the melting transition area [13].

Using DSC, melting properties of the red plinth and reference (pure) beeswax samples were compared. The results from both samples are presented in Fig 2a and b where the heat flow (W/g) is plotted as a function of temperature. DSC system software was used to obtain the onset, major peak and end of the melting transition, while heat of fusion (J/g) was calculated by standard methods: the melting point range is defined as the end temperature of the melting transition subtracted by the onset. The Gauss decomposition of the DSC-curve was applied for more detailed visualization of the melting process of beeswax in the red plinth and the results are presented as an insertion in the Fig. 2b.

Comparative characteristics of melting transition of both samples are presented in Table 1. As one can see from the table and Fig. 2 that the start melting temperature is almost the same while

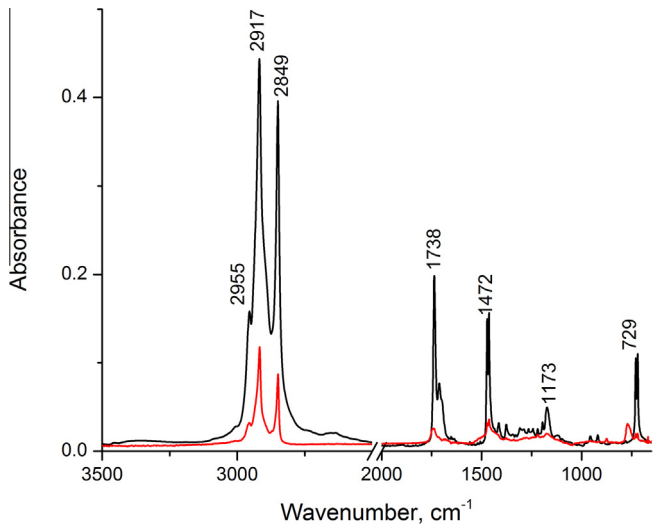

Fig. 4. ATR-FTIR spectra of extracted sample from red plinth (red line) and reference beeswax (black line). (For interpretation of the references to color in this figure legend, the reader is referred to the web version of this article.)

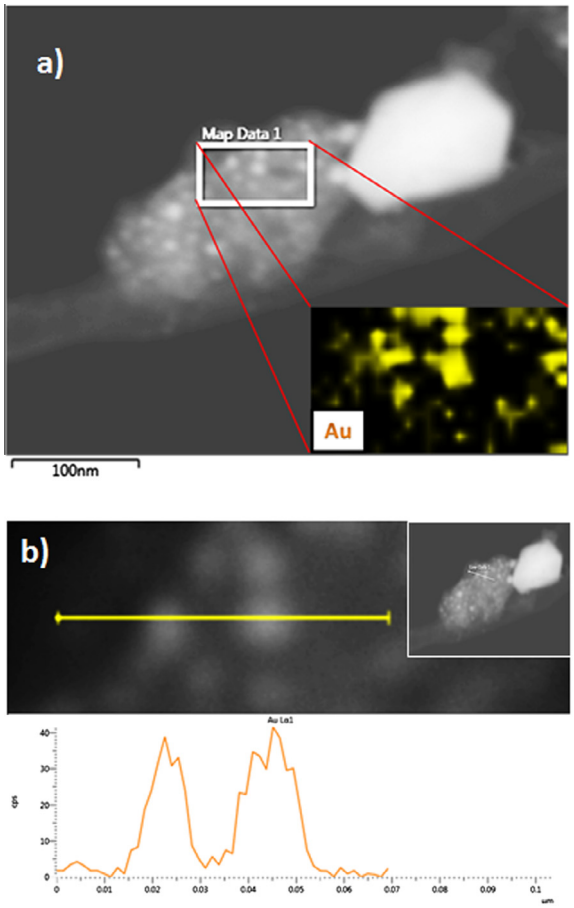

Fig. 5. (a) STEM dark filed image of sample containing Au NPs. EDS elemental mapping shows distribution of Au of the selected area (the insert) and (b) EDS line scan presents the Au profile of two particles across the drawn scanning line.

the end temperature is higher for red plinth sample compared to the referent one. Referent sample reveals two overlapping peaks with the dominant peak (based on the contribution to the total heat of fusion) appearing at the higher end of the temperature range. These peaks probably represent the melting of distinct phases, i.e., fatty acids and wax esters, found in beeswax [11]. The melting transition behavior of red plinth sample is rather different. There is one broad complicated endothermic effect maximizing at about 72 °C and decomposing to 5 peaks when the Gauss fitting procedure was applied. The number of peaks and their location reflect the nature of the chemical components comprising the sample. The multiple peaks evident in the thermogram insertion shown in Fig 2b suggest that the red plinth wax is not a single-phase material. Moreover, the heat of fusion is 6 times less than the one of the referent beeswax sample (Table 1). In fact, the presence of inorganic components in the investigated red plinth sample has an impact on the observed fusion characteristics. The investigated red plinth sample consists of different inorganic materials mainly of natural origin pigment (red ochre), and calcite [3]. In this sample, the presence of the beeswax is in limited quantities and all other components have influence on the fusion characteristics of the beeswax. The addition of inorganic compounds influences in different way on both the melting point position and the heat of fusion [17]. On the other hand, the mechanical properties of different bees waxes were compared. It was found that the melting points represented by DSC method vary in the range of 39–70 °C and the shape and intensity of the melting peak are different for different waxes [11]. It is worth mentioning that the aging of the sample additionally complicates the DSC study in our case. Nevertheless, our DSC results provide solid evidence for the presence of beeswax in the red plinth samples.

FTIR has been considered as one of the most powerful and effective technique to characterize and identify the molecular structure of organic as well as of inorganic materials. The main advantages of FTIR analysis are the speed, accessibility and the minimal required quantity of studied sample which make this technique really crucial in order to study artwork specimens. Due to these exceptional characteristics and the wide range of application for analysis of archaeological and art sites, FTIR spectroscopy has been selected as main analytical method in many different types of artwork [14–16]. A large number of papers have been published, which shows its importance, covering all kinds of specimens and artistic techniques such as paintings [18–20], icons [21–24] pottery [25,26], metal artifacts [6,27], polychromed sculptures [28,29], etc.

ATR FTIR as well as FTIR (in KBr pellet) analysis of solid sample failed to confirm the presence of beeswax since the expected wax amount in the investigated sample is very little and the bands of inorganic components in red paint layer are very strong. The FTIR spectrum of red plinth in KBr pellet was compared with spectra of $CaCO_3$ and red ochre standards (Fig. 3). It was established that the sample was a mixture of $CaCO_3$ (characteristic bands at 2512, 1797, 1427, 876 and 712 cm^{-1}) and red ochre (characteristic bands at 3698, 3621, 3427, 1092, 1032, 1009, 913, 799, 778, 538 and 472 cm^{-1}). The presence of calcium carbonate is most probably due to the calcite formed as a result of the carbonation process which occurs during the drying process of the wall paintings [5].

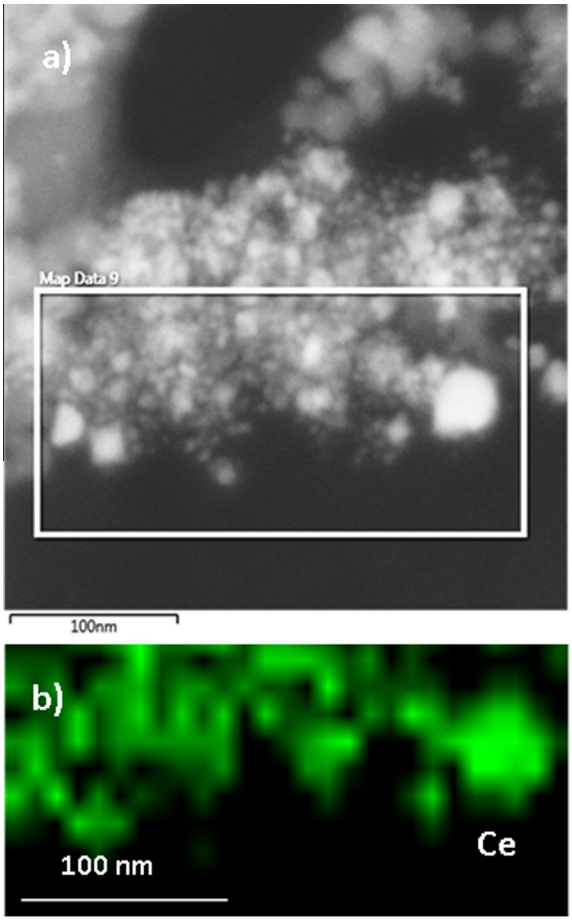

Fig. 6. (a) STEM dark filed image of sample containing CeO_2 NPs and (b) EDS elemental mapping shows distribution of Ce of the selected area in image (a).

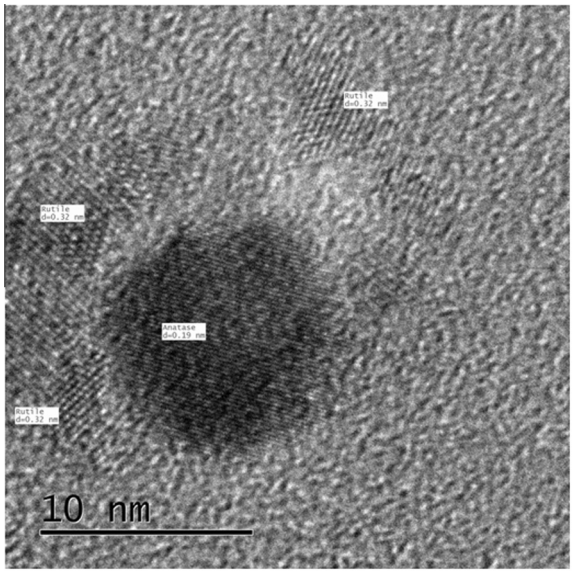

Fig. 7. HR-TEM image with Gatan digital camera showing Anatase NP in the middle surrounded with smaller Rutile NPs.

To confirm the presence of beeswax, the red plinth sample (about 0.20 mg) was extracted with chloroform and analyzed by FTIR. FTIR spectra of red plinth extraction, together with FTIR spectrum of reference beeswax are presented on Fig. 4 Despite the small sample amount there is a good coincidence between FTIR spectra of beeswax and investigated sample. Strong C–H stretching bands in the region 3000–2800 cm^{-1}, stretching C═O band at 1738–1736 cm^{-1}, bending C–H bands at 1472–1463 cm^{-1}, stretching C–O band at 1219–1173 cm^{-1} and torsion C–H bands at 729–719 cm^{-1} are good evidence for the presence of beeswax.

HR-TEM and EDS analyses

In order to establish the chemical composition and particularly the composition of trace elements, red plinth sample was analyzed by EDS in STEM mode. Since the sample was highly non-homogeneous, to guarantee representable results many sites (typically more than 10) from the sample were investigated. The EDS spectra show that the main elements in the red plinth are Ca, O, Fe, Si and Mg. There is also number of elements like Al, Ti, Ce, Au, K, S and P with less than 1 weight (wt)%. Series of HR-TEM analyses were carried out mainly to provide detailed information at micro and nano-scale about the morphology and composition of the studied sample. Interestingly, the HR-TEM study reveals the presence of various nano-size materials in certain areas of the red plinth.

STEM dark filed imaging in Fig. 5a shows presence of Au nanoparticles (on Mg support) in the red plinth. EDS elemental mapping (the insert in Fig. 5a) shows the distribution of Au across the selected area where the Au is 7.5 wt%. The line scan profile (Fig 5b) gives nice Au particles profile matching exactly with the particles where the scanning line was drawn. It can be estimated that the average size of Au particles is in the range of 5–15 nm.

The presence of TiO_2 nanoparticles (NPs) in the form of both Rutile and Anatase was detected in many areas of the red plinth sample. High-resolution TEM image (Fig. 7) shows mixture of different in size TiO_2 NPs. By measuring the crystal lattice spacing it was possible to determine the type of TiO_2 NPs. It was established that 10 nm TiO_2 particles in the middle of Fig. 7 is Anatase with distinctive lattice spacing of 1.9 Å and it is surrounded with much smaller particles with lattice spacing of 3.2 Å typical for Rutile. Another Rutile NPs with very well defined facets of 15 nm and lattice spacing of 3.2 Å is presented in Fig. 8. TiO_2 NPs are one of the most widely used to date commercially available engineered NPs. They are used in paints, pigments, lacquers, plastics, papers, catalysts, cosmetics, fabric coatings, ceramics, printing inks, etc. For some of the traditional uses such as paints and coatings, TiO_2 NPs are incorporated into the bulk material where their tight size control provides a material with enhanced hardness, scrub resistance, and contrast ratio, storage stability and gloss [30,31]. Recently, a lot of interest attracted the application of TiO_2 NPs as photocatalyst in hygienic coatings [32].

Presence of CeO_2 in some selected micro-particles in the red plinth was also detected (Fig. 6). STEM image (Fig. 6a) and EDS elemental mapping (in Fig 6b) show the distribution of CeO_2 NPs across the selected area. The size CeO_2 NPs (ranging from 5 to 50 nm) is less uniform compared to Au NPs.

It is difficult to quantify the total amount of TiO_2, Au and CeO_2 NPs in the red paint since nano-materials are found in very inhomogeneously distributed micro-scale particles across the sample. By EDX elemental analysis of individual micrometer scale particle we found presence of Ti (7.7 wt%), Ce (6.6 wt%) and Au (3.18 wt%) as presented in Table 2. Since CeO_2 could not play a role

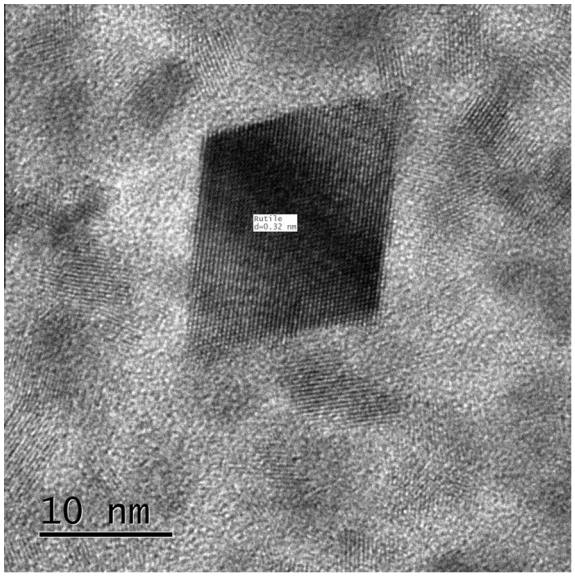

Fig. 8. HR-TEM image with Gatan digital camera showing well faceted Rutile NP.

Table 2
EDX composition in wt% of a micrometer scale particle containing CeO_2 and Au NPs.

Element	wt%
C	24.70
O	37.88
Na	0.67
Mg	0.33
Al	6.82
Si	2.09
S	0.25
K	7.15
Ca	0.63
Ti	7.75
Mn	1.56
Fe	0.39
Ce	6.60
Au	3.18
Total	100.00

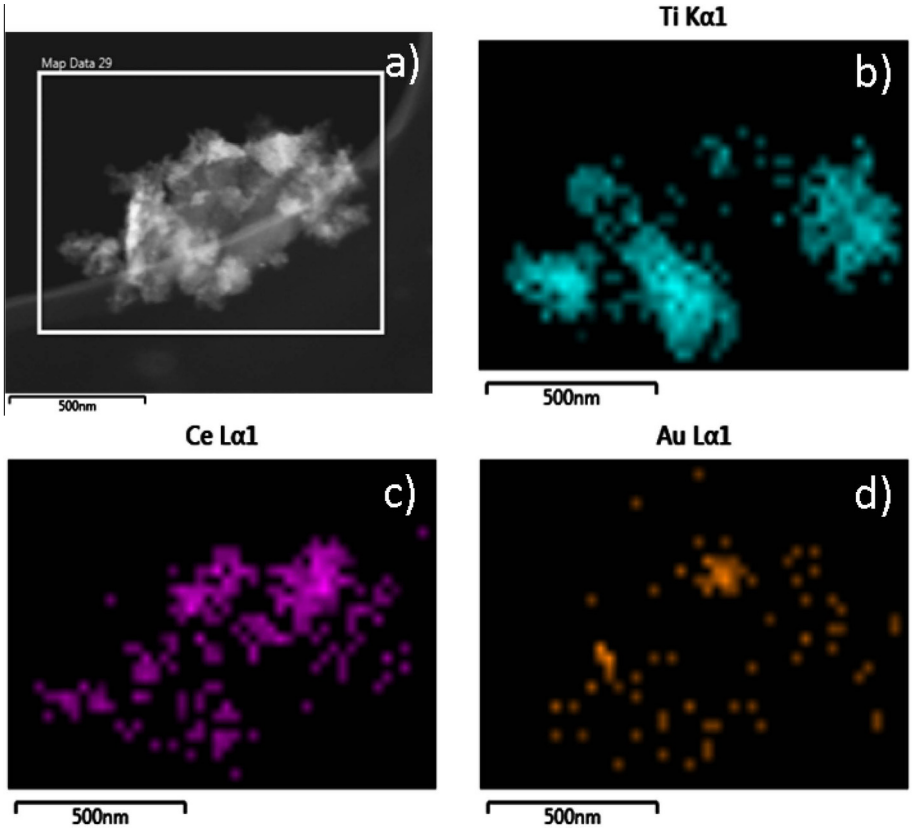

Fig. 9. (a) STEM image of micro-scale particle having CeO_2 and Au NPs on TiO_2 support, (b–d) represent mapping of Ti, Ce and Au, respectively.

as UV-absorber due to the lack of source of UV radiation in the tomb, we believe that redox/oxygen storage properties of CeO_2 might play a role in the very well preserved tomb wall paintings. Interestingly, we found that CeO_2 NPs are always deposited on TiO_2 support which makes CeO_2 stronger catalyser [33]. The elemental mapping presented in Fig 9b–d demonstrates presence of CeO_2 and Au NPs on TiO_2 micro and nano-crystals. We believe that the presence of various NPs is not on purpose since they exist in the nature and were introduced in the sample as a mixture with the other paint components.

Conclusions

Despite the small amount of the investigated sample, the combination of FTIR and DSC successfully confirms the presence of beeswax in Alexandrovo wall paintings samples. The Thracian tomb at Alexandrovo is one of the oldest examples in the world that has paintings executed with wax binder. Whether or not this technique can be referred to as encaustic is still debatable and need further detailed research.

HR-TEM and EDS study reveals the presence of nano-size Au, TiO_2 and CeO_2 particles in certain areas of the red plinth. The presence of these nanomaterials in the sample is not intentional, however it could be a factor contributing to the optical effects and well preservation of the wall paintings used in the Thracian tomb at Alexandrovo.

Acknowledgment

The financial support of this work by the National Science Fund of Bulgaria (Contract K02-15) is gratefully acknowledged.

References

[1] G. Kitov, Archaelogia Bulgarica 2 (2001) 15–29.
[2] Z. Barov, V. Groudeva, M. Karazlateva, K. Kitanov, T. Marinov, in: D. Sounders, J.H. Townsend, S. Woodcock (Eds.), Crossing Conservation, International Institute for Conservation of Historic and Artistic Works, London, 2006, pp. 211–216.
[3] V. Todorov, The Thracian tomb at Aleksandrovo, Interdisziplinäre Forschungen zum Kulturerbe auf der Balkanhalbinsel (2011) 323–334.
[4] D. Giurdzhiiska, Bulg. e-J. Archaeol. 3 (2013) 137–154.
[5] P. Mora, L. Mora, P. Philippot, Conservation of Wall Paintings, Butterworths, London, 1984.
[6] M. Serpico, R. White, in: P. Nicholson, I. Shaw (Eds.), Ancient Egyptian Materials and Technology, British Museum, London, 2000, pp. 390–430.
[7] W. Luo, T. Li, C. Wang, F. Huang, J. Archaeol. Sci. 39 (2012) 1227–1237.
[8] H. Kühn, Stud. Conserv. 2 (1960) 71–81.
[9] B. Ramer, Stud. Conserv. 24 (1979) 1–13.
[10] A. Burmester, Stud. Conserv. 37 (1992) 73–81.
[11] R. Buchwald, M.D. Breed, A.R. Greenberg, J. Exp. Biol. 211 (2008) 121–127.
[12] F. Bernardini, C. Tuniz, A. Coppa, L. Mancini, D. Dreossi, D. Eichert, G. Turco, M. Biasotto, F. Terrasi, N. De Cesare, Q. Hua, V. Levchenko, PLoS ONE 7 (2012) e44904.
[13] U. Knuutinen, A. Norrma, Wax analysis in conservation objects by solubility studies, FTIR and DSC, proceed, in: 15th World Conference on Nondestructive Testings, Roma, 15–21 Oct, 2000.
[14] M.R. Derrick, D. Stulik, J.M. Landry, Infrared Spectroscopy in Conservation Science, Getty Conservation Institute, Los Angeles, 1999.
[15] G. Bitoss, R. Giorgi, M. Mauro, B. Salvadori, L. Dei, Appl. Spectrosc. Rev. 40 (2005) 187–228.
[16] I. Arrizabalaga, O.J. Gomez-Laserna Aramendia, G. Arana, J.M. Madariaga, Spectrochim. Acta A 129 (2014) 259–267, http://dx.doi.org/10.1016/j.saa.2014.03.096.
[17] Z. Liu, D.D.L. Chung, Thermochim. Acta 366 (2001) 135–147.
[18] J. Cuní, P. Cuní, B. Eisen, R. Savizky, J. Bové, Anal. Methods 4 (2012) 659–669.
[19] S. Vahur, A. Teearu, I. Leito, Spectrochim. Acta A 75 (2010) 1061–1072.
[20] S. Akyzuk, T. Akyzuk, G. Emre, A. Gulec, S. Basaran, Spectrochim. Acta A 89 (2012) 74–81.
[21] D. Kovala-Demertzi, L. Papathanasis, R. Mazzeo, M.A. Demertzis, E.A. Varella, S. Prati, J. Cult. Herit. 13 (2012) 107–113.
[22] I.C.A. Sandu, S. Bracci, I. Sandu, M. Lobefaro, Microsc. Res. Tech. 72 (2009) 755.

[23] I.C.A. Sandu, C. Luca, I. Sandu, V. Vasilache, M. Hayashi, Rev. Chem. (Bucuresti) 59 (2008) 384–387.
[24] A. Baciu, Z. Moldovan, I. Bratu, O.F. Măruțoiu, I. Kacsó, I. Glăjar, A. Hernanz, C. Măruțoiu, Curr. Anal. Chem. 6 (2010) 53–59.
[25] D. Barilaro, G. Barone, V. Crupi, D. Majolino, P. Mazzoleni, G. Tigano, V. Venuti, Vib. Spectrosc. 48 (2008) 269–275.
[26] S. Legnaioli, F.A. Garcia, A. Andreotti, E. Bramanti, D.D. Pace, S. Formola, G. Lorenzetti, M. Martini, L. Pardini, E. Ribechini, E. Sibilia, R. Spiniello, V. Palleschi, Spectrochim. Acta A 100 (2013) 144–148.
[27] J. Baeten, K. Romanus, P. Degryse, W. De Clercq, H. Poelman, K. Verbeke, A. Luypaerts, M. Walton, P. Jacobs, D. De Vos, M. Waelkens, Microchem. J. 95 (2010) 227–234.
[28] D. Cauzzi, G. Chiavari, S. Montalbani, D. Melucci, D. Cam, H. Ling, J. Cult. Herit. 14 (2013) 70–75.
[29] A. Sarmiento, M. Pérez-Alonso, M. Olivares, K. Castro, I. Martínez-Arkarazo, L.A. Fernández, J.M. Madariaga, Anal. Bioanal. Chem. 399 (2011) 3601–3611.
[30] B. Kim, M. Murayama, B.P. Colman, M.F. Hochella Jr., J. Environ. Monit. 14 (2012) 1129–1137.
[31] X. Wang, J. Zhang, W. Zhu, L. Shi, J. Shanghai Univ. (English Edition) 11 (2007) 432–436.
[32] V. Jašková, L. Hochmannová, J. Vytřasová, Int. J. Photoenergy (2013) 6 (Article ID 795060).
[33] J.B. Park, J. Graciani, J. Evans, D. Stacchiola, S. Ma, P. Liu, A. Nambu, J.F. Sanz, J. Hrbek, J.A. Rodriguez, PNAS 106 (2009) 4975–4980.